Targeted new membrane addition in the cleavage furrow is a late, separate event in cytokinesis

C. B. Shuster* and D. R. Burgess†

Department of Biology, Boston College, Chestnut Hill, MA 02467, and The Marine Biological Laboratory, Woods Hole, MA O2543

Edited by Lewis G. Tilney, University of Pennsylvania, Philadelphia, PA, and approved January 7, 2002 (received for review July 5, 2001)

Cytokinesis in animal cells is accomplished in part by an actomyosin contractile ring. Recent work on amphibian, *Drosophila*, and *Caenorhabditis elegans* embryos implicates membrane trafficking and delivery as essential for cytokinesis. However, the relative contributions of contractile ring constriction versus membrane insertion to cytokinesis and the temporal relationship between these processes are largely unexplored. Here we monitor secretion of the extracellular matrix protein, hyalin, as a marker for new plasma membrane addition in dividing sea urchin zygotes. We find that new membrane addition occurs specifically in the cleavage furrow late in telophase independent of contractile ring constriction. The directed equatorial deposition of new furrow membrane requires astral microtubules and release of internal stores of Ca^{2+}, but not the presence of a central spindle. Further, cells arrested in M phase do not secrete hyalin, suggesting that mitotic exit is required for new membrane addition. These results demonstrate that astral overlap in equilaterally dividing cells not only serves to specify positioning and contraction of the contractile ring, but also to direct the delivery of new membrane to the furrow as a late, independent event during cytokinesis.

The fundamental mechanics by which chromosomes are segregated into daughter cells during mitosis are highly conserved in eukaryotic cells. The cyclin-dependent kinase-mediated assembly of a microtubule-based mitotic spindle, the antagonistic actions of molecular motors, and the presence of a kinetochore-based mitotic checkpoint are common to all plant, animal, and fungal cells (1). In contrast, a variety of strategies are used to effect the physical partitioning of cytoplasm during cytokinesis (2), which has complicated the understanding of cleavage plane determination and daughter cell separation. Recent advances in model organisms, however, have revealed commonalties suggesting that the mechanisms of cytokinesis in diverse systems are more similar than previously appreciated (3). One component of cytokinesis that may be a requirement for both plant and animal cells is the generation of new plasma membrane (4, 5).

Daughter cell separation in plant cells is driven by the generation of new cell surface at the cleavage plane. A microtubule- and microfilament-based structure termed the phragmoplast is formed at the spindle midzone that mediates the delivery of membrane vesicles that in turn fuse to form the new cell wall (6). Like plant cells, the mitotic apparatus in animal cells also specifies the cleavage plane, but does so by directing the assembly of an actomyosin contractile ring, which provides the contractile force for furrow ingression (7). The role of membrane addition in cytokinesis in most animal cells, however, is less clear.

In large embryonic cells, such as dividing amphibian eggs, the requirement for new membrane addition has been appreciated for some time (8). In these cells, new membrane addition is independent of furrow constriction because inhibition of contractile ring assembly or interference with rho GTPase function does not interfere with membrane addition (8, 9). Additionally, a clear requirement for membrane addition has been demonstrated during *Drosophila* cellularization, where new membrane is added along the ingressing furrow canals (10). Moreover, analyses in *Drosophila*, *Caenorhabditis elegans*, and sea urchin eggs indicate that syntaxins as well as several rab family members are required for successful cellularization or cleavage (11–15). Additionally, mutants of clathrin and large volume sphere (lvsA), two proteins involved in membrane trafficking, also have cytokinesis phenotypes in *Dictyostelium* (16, 17). Together, these findings suggest that membrane trafficking and addition may be a universal requirement for cytokinesis in all eukaryotic cells.

In many respects, however, furrow ingression in *Xenopus* eggs and cellularization in *Drosophila* embryos represent specialized forms of cytokinesis. Whether new membrane addition is under the same spatial and temporal constraints in cells with more conventional relationships between the mitotic apparatus and contractile ring remains largely unknown. In this article, we investigate the addition of new surface area in dividing sea urchin eggs. Using the exocytosis of an extracellular membrane protein as a marker for new membrane addition, we report that astral microtubules direct the polarized delivery of hyalin to the cleavage plane independently of the central spindle or contractile ring function. Interference with astral microtubule growth or contact with the cell cortex, calcium-mediated exocytosis, or mitotic exit inhibits new membrane addition at the cleavage plane. Together these results suggest that like plant cells, microtubules emanating from the spindle poles direct the delivery of new membrane to the division site, in a manner similar to, but temporally distinct from, the positioning and induction of the contractile ring.

Materials and Methods

Embryo Culture. The sea urchins *Lytechinus pictus* and *Strongylocentrotus purpuratus* were obtained from Marinus (Long Beach, CA) and *Lytechinus variegatus* were obtained from Susan Decker (Davie, FL); and animals were maintained in fresh running seawater (SW) at the Marine Biological Laboratory. Gametes were obtained by intracoelemic injection of 0.5 M KCl, and after fertilization, zygotes were stripped of their fertilization membranes and hyalin layers by passage through nitex and cultured in calcium-free SW (CaFSW) at 17°C (*L. variegatus* was cultured at 24°C). Glycine (1 M) was used to strip the fertilization membranes and hyalin from *S. purpuratus* eggs before culture in CaFSW. To observe hyalin deposition during cell division, cells were cultured in CaFSW until nuclear envelope breakdown (NEB) of the first division (≈60 min). Cells were then transferred to normal SW containing 2–5 μg/ml cytochalasin D (CDSW), and placed in a chamber slide for observation. To examine the dependence of microtubules on equatorial hyalin deposition, cells were fertilized and cultured in CaFSW until

This paper was submitted directly (Track II) to the PNAS office.

Abbreviations: BFA, brefeldin A; SW, seawater; CaFSW, calcium-free SW; CD, cytochalasin D; CDSW, cytochalasin D seawater; NEB, nuclear envelope breakdown; DIC, differential interference contrast.

*Present address: Department of Biology, New Mexico State University, Las Cruces, NM 88003.

†To whom reprint requests should be addressed. E-mail: david.burgess@bc.edu.

The publication costs of this article were defrayed in part by page charge payment. This article must therefore be hereby marked "*advertisement*" in accordance with 18 U.S.C. §1734 solely to indicate this fact.

NEB as described above. Cells were then transferred into CDSW containing either 10 mM nocodazole (Sigma) or 50 mM ethyl carbamate (urethane; Sigma).

For hyalin localization, cells were fixed for 20 min in CaFSW containing 5% formaldehyde. Cells were then briefly incubated in a 1:50 dilution of monoclonal antihyalin (provided by Gary Wessel, Brown University, Providence, RI; ref. 18), and bound antibody was detected with rhodamine anti-mouse IgG (Chemicon). To differentiate the plasma membrane from hyalin in CD-treated cells, 1 μM FM1–43 was included in the CDSW and visualized by epifluorescence microscopy.

To analyze the effect of brefeldin A (BFA) on cell division and hyalin secretion, zygotes were transferred 10 min postfertilization into CaFSW containing 15 or 25 μg/ml BFA (Sigma). After NEB, treated cells were either left in BFA/CaFSW or transferred to CDSW containing BFA. After cleavage of control zygotes, treated cells were scored for cytokinesis and hyalin ring formation, respectively.

Microinjection and Micromanipulation. To examine hyalin deposition in M phase-arrested cells, sea urchin blastomeres were injected with human mad2 (hmad2, provided by Marc Kirschner, Harvard Medical School, Boston) or His-tagged Δ90 cyclin B. Nondegradable cyclin B (Δ90 cyclin B) was expressed in bacteria as described (19). Both proteins were purified by using His-bind nickel agarose (Novagen). To aid in tetramer formation, hmad2 was purified in the presence of 4 M urea and dialyzed step-wise into 10 mM Hepes, 100 mM KCl, 1 mM $MgCl_2$, 1 M DTT, and 1 mM EGTA, pH 7.7. All recombinant proteins were dialyzed into injection buffer (150 mM potassium aspartate/10 mM Hepes, pH 7.0), concentrated to 10–15 mg/ml, clarified, and stored on ice before injection. For microinjection experiments, embryos were cultured in CaFSW until NEB of the second division, and then transferred into CDSW. One blastomere was injected with the other blastomere serving as an uninjected control, and injection volumes varied between 0.5% and 2% of cell volume. Cells were cultured for an additional 40 min and then scored for the accumulation of hyalin on the surface of the cells, and mitotic arrest was monitored by using 1 μg/ml Hoescht 33342 (Molecular Probes).

To interfere with calcium-dependent exocytosis, sea urchin eggs were fertilized, cultured until NEB, and transferred into CDSW. Cells were then injected with 10 mg/ml heparin in injection buffer, which also contained 10 μM fluorescein dextran to mark injected zygotes. Control injections were performed with 10 mg/ml de-*N*-sulfated heparin, which does not interfere with inositol trisphosphate-mediated calcium transients (20).

Needle manipulations of sea urchin eggs were performed as described (19). Nomarski differential interference contrast (DIC) or fluorescence images were recorded on a Nikon TE 200 microscope, equipped with a Uniblitz (Vincent Associates, Rochester, NY) shuttered tungsten lamp and a shuttered EFOS (Mississauga, Ontario, Canada) X-cite metal halide illuminator, with a Hamamatsu (Ichinocho, Japan) Orca digital charge-coupled device camera, all controlled with a Universal Imaging (Media, PA) Metamorph system. Figures were prepared by using Adobe PHOTOSHOP software.

Results

Hyalin Serves as a Marker for New Membrane Addition. To study new membrane addition, we followed the secretion and deposition of the extracellular matrix protein, hyalin, in the dividing sea urchin zygote. Hyalin (18) is released in a calcium- and SNARE-dependent manner into the extracellular milieu upon fertilization, where it immediately precipitates in place in the presence of extracellular calcium to form an adhesive and immobile extracellular matrix (21) (Fig. 1*A*). Culture of zygotes in the absence of calcium dramatically reduced the amount of hyalin on the cell surface and resulted in poorly adherant blastomeres (Fig. 1*B*). However, because cells continually secrete hyalin throughout early cleavage divisions (22), hyalin deposition as well as cadherin-mediated cell adhesion can be restored simply by switching the cells back into normal calcium-containing SW (Fig. 1*C*). Based on these properties, we reasoned that extracellular, Ca^{2+}-dependent hyalin deposition represented a potential marker for new membrane addition during cell division.

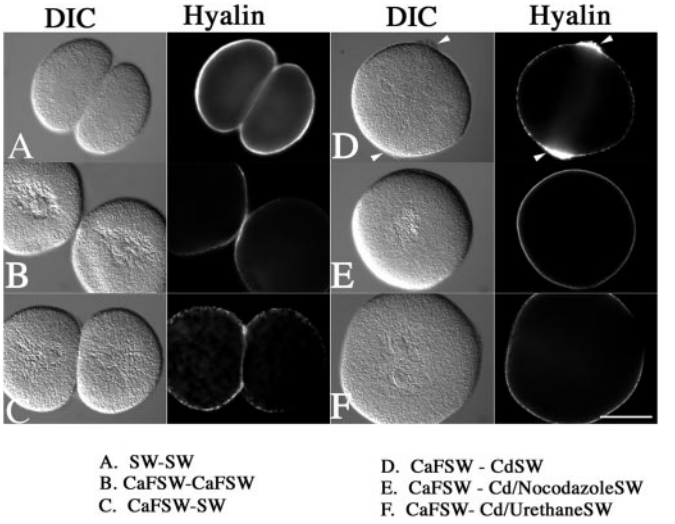

Fig. 1. Manipulation of SW composition and cytoskeletal drugs to examine secretion during cell division. *L. pictus* eggs were fertilized, stripped of their fertilization membranes, and cultured in either normal SW (*A*) or CaFSW (*B*) through the first cleavage. Alternatively, cells were cultured in CaFSW until NEB, and then transferred into normal SW (*C*) or CDSW (*D*) to inhibit cytokinesis. Additionally, microtubules were disrupted with either 10 μM nocodazole (*E*) or 50 mM urethane (*F*). Cells were then fixed and processed for hyalin localization. Arrows denote the accumulation of hyalin at the cleavage plane in *D*. (Bar = 50 μm.)

Membrane addition during cytokinesis in large amphibian eggs continues in the absence of a functional contractile ring (8, 9). To determine whether hyalin deposition at the cell surface of sea urchin eggs behaves in a similar manner, *L. pictus* eggs were fertilized and cultured in CaFSW to prevent hyalin precipitation (but not secretion) on the cell surface. Upon NEB, cells were transferred into normal (9 mM Ca^{2+}) CDSW (Fig. 1*D*). Whereas cells transferred into CDCaFSW were binucleate with a thin extracellular matrix uniformly distributed on the cell surface (data not shown), cells transferred into CDSW consistently displayed a thick circumferential ring of extracellular, insoluble material localized at the equatorial zone between the two interphase nuclei (Fig. 1*D*, arrows). These equatorial rings were enriched with hyalin by immunofluorescence, and similar rings of extracellular matrix could be detected in other species treated in this manner (*Arbacia punctulata, L. variegatus*, *S. purpuratus*), with some variation in the amount of material deposited at the equator. The circumferential hyalin rings were on average 25 μm in width, but varied between 16 and 33 μm. Optimal conditions were obtained when lower concentrations of cytochalasin were used (2–5 μg/ml), which allowed for the establishment of cleavage furrows that froze or retracted shortly after initiation.

Newly secreted hyalin could be visualized easily by DIC in either normal dividing cells or CD-treated cells, and subsequent immunolocalization confirmed that this extracellular, insoluble material was composed of hyalin (Fig. 2). While a thin layer of hyalin was present over the entire cell surface, hyalin was enriched in the ingressing furrow of normal dividing cells (Fig. 2 *A* and *B*), as well as the equatorial zone of CD-treated cells

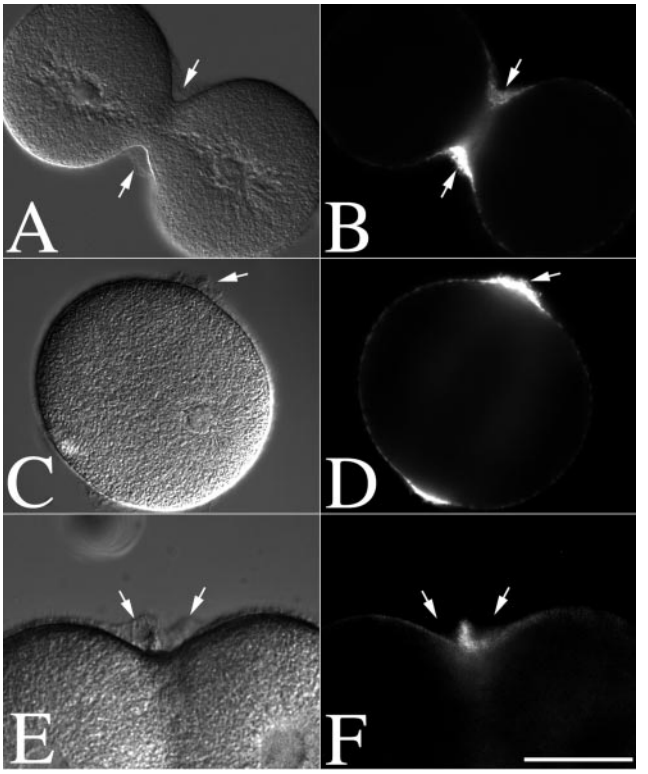

Fig. 2. Hyalin and membrane accumulation at the cleavage plane of dividing and CD-treated zygotes. *L. pictus* eggs were fertilized, stripped of their fertilization membranes, and cultured in CaFSW. At NEB, zygotes were transferred to normal SW (*A* and *B*) or CDSW (*C–F*). Cells were then fixed and processed for hyalin localization (*A–D*). Alternatively, cells cultured in CaFSW were transferred into CDSW containing 1 μM FM1–43 to directly visualize the plasma membrane (*E* and *F*). Arrows denote the position of hyalin. (Bar = 50 μm.)

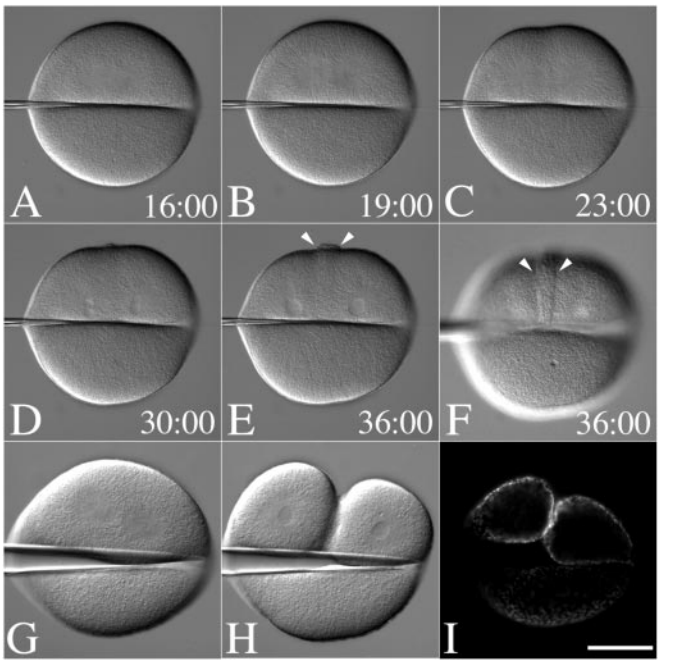

Fig. 3. Positional regulation of secretion by the mitotic apparatus. (*A–F*) Fertilized *L. pictus* eggs were cultured in CaFSW. Just before NEB, cells were transferred to CDSW. A bent microneedle was gently applied to the surface of the egg, displacing the spindle toward one side of the flattened cell. After anaphase onset (*A*), the astral microtubules extended toward the cortex (*B*), and a shallow furrow forms at the midzone between the two aster centers (*C*). Hyalin appears at the surface during nuclear envelope reformation (*D*), which accumulates further in the cleavage-arrested cell (*E* and *F*) (see Movie 1). Arrows denote the zone of membrane addition. (*G–I*) Just before NEB, cells were cultured on a protamine sulfate-coated coverslip. A bent microneedle was gently applied to the surface of the egg, displacing the spindle toward one side of the flattened cell (*G* and *H*). Cells were fixed in place, and after fixation, the needle was removed, and the coverslip was processed for hyalin immunolocalization (*I*). (Bar = 50 μm.)

where the furrow normally forms in the absence of cytochalasin (Fig. 2 *C* and *D*). Observation of both living and fixed, CD-treated cells also revealed the concomitant appearance of both hyalin and small membrane blebs or projections at the cleavage plane. To confirm accumulation of hyalin at the cell equator and differentiate it from projections in the plasma membrane, cells cultured in CaFSW were transferred into CDSW containing the membrane dye FM1–43. FM1–43 staining of CD-treated cells revealed that while small membrane buckles or protrusions could be seen in CD-treated cells (Fig. 1*F*), hyalin appeared by DIC as untextured or smooth whereas membrane projections and microvilli were clearly textured and distinct from the smooth hyalin layer (Fig. 2 *E* and *F*). These FM1–43-staining projections resulted in an overall increase of dye fluorescence at the cell equator (Fig. 2*F*), and occurred regardless of whether there was calcium present in the CDSW (data not shown), and thus were not likely to be a consequence of hyalin deposition.

Astral Microtubules Direct Hyalin and Membrane Accumulation at the Cleavage Plane. To determine whether there was a requirement of microtubules for the equatorial deposition of hyalin, cells were cultured in CaFSW until NEB, and then transferred into CDSW and microtubule inhibitors (Fig. 1 *E* and *F*). Whereas transfer of eggs from CaFSW to CDSW resulted in the accumulation of hyalin at the normal site of the cleavage furrow (Figs. 1*D* and 2*D*), treatment with 10 μM nocodazole completely inhibited new hyalin secretion in the presumptive furrow region (Fig. 1*E*). Urethane (50 mM), which destabilizes astral microtubules without affecting the spindle assembly or chromosome segregation (23), also inhibited equatorial hyalin deposition (Fig. 1*F*).

The temporal and spatial dynamics of hyalin secretion and membrane fold formation during cytokinesis were further explored by examining eggs where the mitotic apparatus was physically displaced by micromanipulation. By applying a microneedle onto the surface of a dividing egg, the mitotic apparatus can be displaced to one side such that a cleavage furrow forms only on the side of the egg containing the spindle (Fig. 3 *G* and *H*) (24). Cells were transferred into CDSW after NEB and manipulated with a needle, and hyalin accumulation was followed by time-lapse microscopy (Fig. 3; Movie 1, which is available as supporting information on the PNAS web site, www.pnas.org). By 19 min past NEB, anaphase asters were visible (Fig. 3*B*), and a shallow and incomplete cleavage furrow was observed 4 min later (Fig. 3*C*) in the region of astral overlap. Hyalin deposition was first visible at the time of nuclear envelope reformation (Fig. 3*D*) when control eggs were completing cytokinesis (not shown). And while astral fibers could be seen extending from the asters into the enucleate side of the cell, the hyalin band was detected only on the side of the cell containing the mitotic apparatus (Fig. 3 *E* and *F*, arrows). To confirm that hyalin secretion was enriched in the furrows of cells manipulated in this fashion, dividing eggs were manipulated such that the spindle was displaced toward one side, and the cell was fixed with the needle in place and processed for hyalin immunolocalization (Fig. 3*I*). As with the unmanipulated, CD-treated cells, hyalin was detected all over the surface of the egg, but was enriched on the side of the cell containing the spindle and the ingressing furrow (Fig. 3*I*).

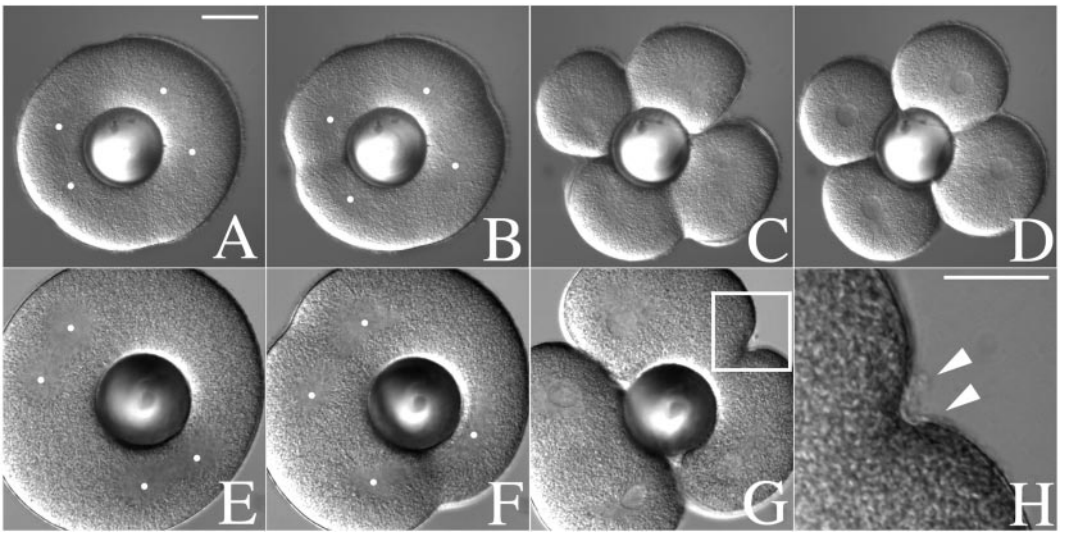

Fig. 4. Mitotic asters direct both cleavage plane determination and new membrane addition. The first cleavage of *L. pictus* embryos was suppressed by culturing zygotes in CaFSW containing 50 mM urethane after NEB. Shortly before NEB of the second division, cells were transferred into a chamber containing normal SW, and a glass ball was gently pressed down onto the surface of the egg, displacing the two spindles to opposite sides of the cell. In the absence of cytochalasin (*A–D*), cleavage furrows formed both at the midzone between overlapping asters of the same spindle, as well as between the asters of adjacent spindles. In the presence of 2 μg/ml CD (*E–H*), furrows initiated by overlapping asters over the metaphase plate of each spindle progressed to completion (*G*). Furrows induced by overlapping asters from different spindles failed to initiate or retracted (*G*). However, hyalin deposition at these retracted furrows was not affected (*H*, arrows). Dots indicate the approximate location of the aster centers. The image shown in *H* represents the region highlighted in *G*. (Bar = 25 μm.)

In the now classic "torus" experiments, Rappaport (25) established that cleavage furrows are induced at zones of astral fiber overlap, regardless of whether there is an intervening central spindle. To determine whether new membrane addition in the furrow required only astral overlap (as is the case for contractile ring induction), we combined manipulation of hyalin solubility with a modified version of Rappaport's torus experiment (Fig. 4). Binucleate cells were generated by suppressing the first cleavage (but not mitosis) with 50 mM urethane. Shortly before NEB of the second division, binucleate cells were transferred into normal SW and a glass ball was gently pushed through the center of the cell to isolate the two spindles (Fig. 4*A*). After anaphase onset, cleavage furrows formed initially at the midzone of each spindle (Fig. 4*B*), and later at the site of astral overlap between the different spindles (Fig. 4 *B* and *C*), resulting in four blastomeres (Fig. 4*D*). To visualize hyalin deposition in these "secondary" furrows, cells were transferred into SW containing very low doses of cytochalasin (1–2 μg/ml), which disrupts or slows furrows induced by overlapping asters from two distinct spindles (Fig. 4 *E–H*). Under these conditions, hyalin was observed by DIC in the shallow furrows induced at the midzone between the asters from unrelated spindles, indicating that astral microtubules could not only direct the position of the cleavage furrow independently of a central spindle (25), but also direct the secretion of hyalin to the cleavage plane.

New Membrane Addition Requires Mitotic Exit and Ca^{2+}-Dependent Exocytosis. The timing of hyalin deposition on the cell surface (Fig. 3; Movie 1) suggested that new membrane addition was a late event in cytokinesis. To explore the cell cycle dependence of new membrane addition, CD-treated eggs were arrested in metaphase by injection of human mad2 (26) or arrested in anaphase with nondegradable cyclin B (Δ90 cyclin B) (27). Because the mitotic asters of these arrested cells do not elongate and contact the cell surface (19), microneedles were applied to the surface of these cells as shown in Fig. 3, and cells were assayed for their ability to form hyalin rings. No hyalin deposition or membrane projections could be detected in mad2- (n = 24) or Δ90 cyclin-arrested cells (n = 23) (data not shown), indicating that hyalin secretion depended on anaphase and mitotic exit.

In sea urchin eggs, membrane delivery during exocytosis and plasma membrane wound healing has been shown previously to depend on release of internal stores of calcium ions (28, 29). Zygotes were transferred into CDSW and injected with heparin during metaphase, a potent antagonist of inositol trisphosphate-dependent calcium channels in sea urchin eggs (20). The dose of heparin used (100–200 μg/ml final concentration) delayed, but did not block anaphase onset (30), and shallow furrows formed in both control (Fig. 5*A*) and heparin-injected zygotes (Fig. 5*B*). However, 93% of heparin-injected cells (n = 81) had no visible hyalin rings or membrane folds (Fig. 5*B*). In contrast, hyalin rings were detected in 80% of cells injected with de-*N*-sulfated heparin (n = 36), which does not affect inositol trisphosphate-mediated calcium signaling or in 86% of uninjected zygotes (n = 71) (data not shown). Therefore, hyalin deposition at the cleavage plane was likely mediated by Ca^{2+}-dependent exocytosis of hyalin-containing vesicles.

The inhibitory effect of heparin on hyalin deposition at the cleavage furrow suggested that the source of hyalin was intracellular, Golgi-derived vesicles. To determine whether BFA, which disrupts endoplasmic reticulum to Golgi transport (31), effects hyalin secretion or cytokinesis in sea urchin embryos, fertilized eggs were cultured in CaFSW and transferred into CaFSW containing BFA 10 min postfertilization and cultured through the second division at concentrations (15 and 25 μg/ml) previously reported to inhibit cytokinesis in *C. elegans* embryos (15). While the concentrations of BFA used were 3- to 5-fold higher than what is required to disrupt Golgi structure in the epithelial cells of sea urchin blastulae (32), we found that BFA had no discernable effect on the first or second cell divisions, with more than 93% of treated cells (at either concentration) initiating and completing cleavage (n = 100 for each treatment). Similarly, cells transferred from BFA-SW into BFA-CDSW (Fig. 5 *C* and *D*) formed hyalin rings identical to those observed in controls (Fig. 5*A*).

Discussion

The striking similarities between polarized hyalin secretion in dividing sea urchin eggs and new cell wall assembly in dividing

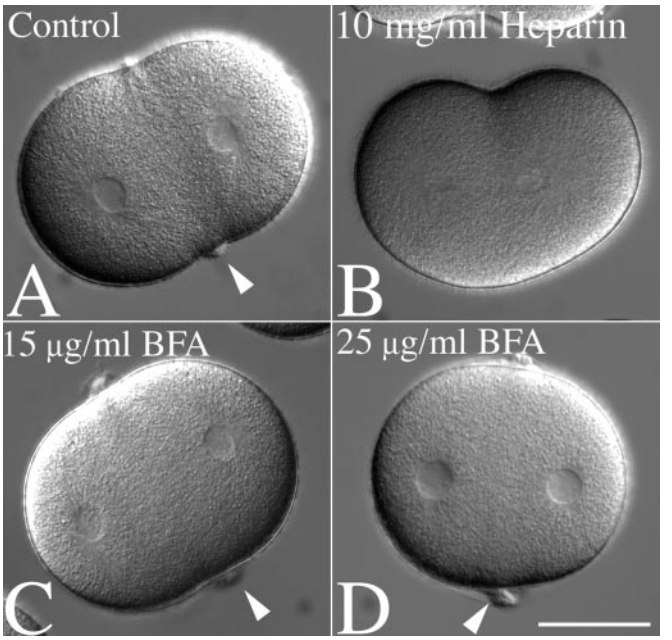

Fig. 5. Equatorial hyalin secretion during cell division requires Ca^{2+}-mediated exocytosis but is insensitive to BFA. (*A* and *B*) *L. pictus* zygotes were cultured in CaFSW until NEB, and then transferred into a chamber containing 2 μg/ml CD in normal SW. Cells were then injected with 10 mg/ml heparin, and injected cells were identified by including fluorescein-dextran in the injection buffer (not shown). Cleavage furrows were initiated in both injected and uninjected cells, but the equatorial accumulation of hyalin observed in control cells (*A*, arrows) was absent in heparin-injected cells (*B*). (*C* and *D*) To determine whether BFA affects hyalin deposition, zygotes were transferred into CaFSW containing 15 or 25 μg/ml BFA (*C* and *D*, respectively), and after NEB, transferred into CDSW containing BFA. Arrows denote the equatorial hyalin rings found at the surface of cleavage-arrested cells. (Bar = 50 μm.)

plant cells lends further support to the notion that new membrane addition is a universal component of cytokinesis in all eukaryotic cells. In this article, we have taken advantage of the calcium-dependent solubility of a secreted extracellular matrix protein to study new membrane insertion during cytokinesis. By tracking new hyalin deposition after NEB, our data demonstrate that the late cleavage furrow is the primary site of membrane addition. Furthermore, membrane addition depends on microtubules, Ca^{2+}-dependent exocytosis, and mitotic exit but is independent of the actin-based contractile ring. New membrane addition has been reported in the furrows of *C. elegans* blastomeres by using the membrane-impermeant dye FM1–43 (15). We also find that FM1–43 accumulates at the equator of CD-treated cells by labeling plasma membrane folds that appear in CD-arrested furrows. Thus, by following both hyalin deposition and FM1–43 labeling of the plasma membrane, we have unambiguously marked the late furrow as the site of membrane insertion during cytokinesis.

The idea that new surface must be generated during cytokinesis dates back to the earliest hypotheses concerning the mechanics of cell division (33), but the requirement for additional surface area, as well as the source of membrane, remains a subject of debate. It has been widely suggested that microvilli, which increase the surface area of sea urchin eggs 4-fold (34), might easily provide the required increase in surface area during cytokinesis. However, measurements of microvillar length through the cell cycle indicate that microvilli are not a likely source of membrane (34, 35). The appearance of new hyalin at the cell surface after mitotic exit (Figs. 1–4), as well as the dependence of hyalin secretion on calcium-dependent exocytosis (Fig. 5), is consistent with observations in *Xenopus* (8, 36–38) and *Drosophila* (10, 39) indicating that a major source of new membrane is derived from internal stores. BFA has been shown to interfere with the final stages of cytokinesis in *C. elegans* blastomeres (15), but had no discernable effect on either cytokinesis or hyalin secretion in sea urchin eggs (Fig. 5), perhaps reflecting the presence of large stores of secretory vesicles formed during oogenesis. Thus, while new membrane addition alone is insufficient to drive furrowing in the absence of a functional contractile ring (Fig. 3; refs. 8 and 9), membrane addition appears to be an important component of cytokinesis in all embryonic cells where the relatively poor surface to volume ratio dictates a need for additional surface area.

Cytokinesis in animal cells may be temporally subdivided into three phases: (*i*) cleavage plane determination, (*ii*) contractile ring assembly, constriction, and disassembly, and (*iii*) midbody formation and abscission. Although it remains to be determined whether these are, indeed, distinct phases or part of a continuum, it appears that membrane addition is a late and separate event, occurring during the final phase of cytokinesis. Time-lapse observation of CD-arrested cells indicates that hyalin secretion at the cleavage plane was coincident with nuclear envelope reformation (Fig. 3, Movie 1) and the completion of cytokinesis in control cells. We found that although mitotic exit is not a direct requirement for cleavage furrow initiation in sea urchin blastomeres (19), membrane addition requires mitotic exit and accompanies the late stages of cytokinesis in sea urchin eggs. Furthermore, new membrane addition and nuclear envelope reformation may well be linked, because inactivation of syntaxin 1 in *C. elegans* disrupts both cytokinesis and nuclear envelope reformation (14).

New membrane addition during cytokinesis requires microtubules in both plant and animal cells, yet the spatial relationship between microtubule organization and membrane insertion has not been clearly established in most animal cells. The animal cell models for membrane addition used to date, namely dividing amphibian eggs and early *Drosophila* embryos, represent more specialized forms of cytokinesis, with unilateral furrows that continue to ingress through the following cell cycle, and an exaggerated requirement for new membrane. In both cases, membrane addition occurs along the lateral walls of these elongate furrows (10, 36), and the microtubules that mediate new surface generation differ greatly from the anaphase-telophase microtubule arrays seen in other animal cells (10, 37). In contrast, new membrane addition in sea urchin eggs is facilitated by overlapping asters that specify the cleavage plane after anaphase onset (Figs. 3 and 4), and thus more closely resemble the likely scenario in other animal cells. In smaller somatic cells, the central spindle (as opposed to the astral microtubules) specifies the cleavage plane (40) and is also required for the completion of cytokinesis (3). And although the central spindle is neither required for cleavage furrow initiation or new membrane addition in sea urchin eggs (Fig. 4), microtubules are required for abscission (41), perhaps reflecting a requirement for new membrane addition at the furrow. And in light of evidence that kinesin is required for the recruitment of exocytotic vesicles during plasma membrane wound healing (29), it is tempting to speculate that delivery of new membrane to the cleavage furrow is driven by related plus end-directed microtubule motors. Thus, in both urchin eggs and somatic cells, the coordination of membrane addition may represent the predominant function of the late mitotic apparatus.

We thank Gary Wessel for the antihyalin antibodies and Marc Kirschner for the hmad2 expression plasmid. This work was supported by National Institutes of Health Grant GM 40086 awarded to D.R.B.

1. Wittmann, T., Hyman, A. & Desai, A. (2001) *Nat. Cell Biol.* **3,** E28–E34.
2. Field, C., Li, R. & Oegema, K. (1999) *Curr. Opin. Cell Biol.* **11,** 68–80.
3. Glotzer, M. (2001) *Annu. Rev. Cell Dev. Biol.* **17,** 351–386.
4. O'Halloran, T. J. (2000) *Traffic* **1,** 921–926.
5. Straight, A. F. & Field, C. M. (2000) *Curr. Biol.* **10,** R760–R770.
6. Smith, L. G. (1999) *Curr. Opin. Plant Biol.* **2,** 447–453.
7. Rappaport, R. (1996) *Cytokinesis in Animal Cells* (Cambridge Univ. Press, Cambridge, U.K.).
8. Bluemink, J. G. & de Laat, S. W. (1973) *J. Cell Biol.* **59,** 89–108.
9. Drechsel, D. N., Hyman, A. A., Hall, A. & Glotzer, M. (1997) *Curr. Biol.* **7,** 12–23.
10. Lecuit, T. & Wieschaus, E. (2000) *J. Cell Biol.* **150,** 849–860.
11. Burgess, R. W., Deitcher, D. L. & Schwarz, T. L. (1997) *J. Cell Biol.* **138,** 861–875.
12. Conner, S. D. & Wessel, G. M. (1999) *Mol. Biol Cell* **10,** 2735–2743.
13. Conner, S. D. & Wessel, G. M. (2000) *FASEB J.* **14,** 1559–1566.
14. Jantsch-Plunger, V. & Glotzer, M. (1999) *Curr. Biol.* **9,** 738–745.
15. Skop, A. R., Bergmann, D., Mohler, W. A. & White, J. G. (2001) *Curr. Biol.* **11,** 735–746.
16. Kwak, E., Gerald, N., Larochelle, D. A., Vithalani, K. K., Niswonger, M. L., Maready, M. & De Lozanne, A. (1999) *Mol. Biol. Cell* **10,** 4429–4439.
17. Niswonger, M. L. & O'Halloran, T. J. (1997) *Proc. Natl. Acad. Sci. USA* **94,** 8575–8578.
18. Wessel, G. M., Berg, L., Adelson, D. L., Cannon, G. & McClay, D. R. (1998) *Dev. Biol.* **193,** 115–126.
19. Shuster, C. B. & Burgess, D. R. (1999) *J. Cell Biol.* **146,** 981–992.
20. Ciapa, B., Pesando, D., Wilding, M. & Whitaker, M. (1994) *Nature (London)* **368,** 875–878.
21. McClay, D. R. & Fink, R. D. (1982) *Dev. Biol.* **92,** 285–293.
22. Kane, R. E. (1973) *Exp. Cell Res.* **81,** 301–311.
23. Rappaport, R. (1971) *J. Exp. Zool.* **176,** 249–255.
24. Rappaport, R. & Ebstein, R. P. (1965) *J. Exp. Zool.* **158,** 373–382.
25. Rappaport, R. (1961) *J. Exp. Zool.* **148,** 81–89.
26. Li, Y., Gorbea, C., Mahaffey, D., Rechsteiner, M. & Benezra, R. (1997) *Proc. Natl. Acad. Sci. USA* **94,** 12431–12436.
27. Holloway, S. L., Glotzer, M., King, R. W. & Murray, A. W. (1993) *Cell* **73,** 1393–1402.
28. Steinhardt, R. A., Bi, G. & Alderton, J. M. (1994) *Science* **263,** 390–393.
29. Bi, G. Q., Morris, R. L., Liao, G., Alderton, J. M., Scholey, J. M. & Steinhardt, R. A. (1997) *J. Cell Biol.* **138,** 999–1008.
30. Groigno, L. & Whitaker, M. (1998) *Cell* **92,** 193–204.
31. Orci, L., Tagaya, M., Amherdt, M., Perrelet, A., Donaldson, J. G., Lippincott-Schwartz, J., Klausner, R. D. & Rothman, J. E. (1991) *Cell* **64,** 1183–1195.
32. Terasaki, M. (2000) *Mol. Biol. Cell* **11,** 897–914.
33. Schechtman, A. M. (1937) *Science* **85,** 222–223.
34. Schroeder, T. E. (1981) in *Cytoskeletal Elements and Plasma Membrane Organization*, eds. Poste, G. & Nicolson, G. L. (Elsevier/North–Holland, Amsterdam), pp. 170–216.
35. Wong, G. K., Allen, P. G. & Begg, D. A. (1997) *Cell Motil. Cytoskeleton* **36,** 30–42.
36. Byers, T. J. & Armstrong, P. B. (1986) *J. Cell Biol.* **102,** 2176–2184.
37. Danilchik, M. V., Funk, W. C., Brown, E. E. & Larkin, K. (1998) *Dev. Biol.* **194,** 47–60.
38. Ohshima, H. & Kubota, T. (1985) *J. Embryol. Exp. Morphol.* **85,** 21–31.
39. Sisson, J. C., Field, C., Ventura, R., Royou, A. & Sullivan, W. (2000) *J. Cell Biol.* **151,** 905–918.
40. Cao, L.-G. & Wang, Y.-L. (1996) *Mol. Biol. Cell* **7,** 225–232.
41. Larkin, K. & Danilchik, M. V. (1999) *Dev. Biol.* **214,** 215–226.